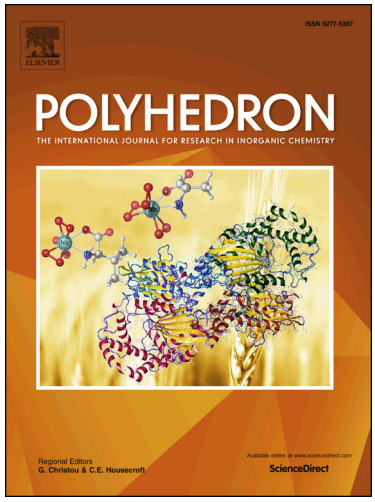

Metal-chelating properties and antiviral activity of some 2-hydroxyphenyl amides

M. Carcelli, E. Fisicaro, C. Compari, L. Contardi, D. Rogolino, C. Solinas, A. Stevaert, L. Naesens

PII: S0277-5387(17)30220-6
DOI: http://dx.doi.org/10.1016/j.poly.2017.03.032
Reference: POLY 12547

To appear in: *Polyhedron*

Received Date: 27 January 2017
Revised Date: 17 March 2017
Accepted Date: 19 March 2017

Please cite this article as: M. Carcelli, E. Fisicaro, C. Compari, L. Contardi, D. Rogolino, C. Solinas, A. Stevaert, L. Naesens, Metal-chelating properties and antiviral activity of some 2-hydroxyphenyl amides, *Polyhedron* (2017), doi: http://dx.doi.org/10.1016/j.poly.2017.03.032

Metal-chelating properties and antiviral activity of some 2-hydroxyphenyl amides

M. Carcelli,*[a,b] E. Fisicaro,[c] C. Compari,[c] L. Contardi,[c] D. Rogolino,[a,b] C. Solinas,[d] A. Stevaert,[e] L. Naesens[e]

[a]Dipartimento di Scienze Chimiche, della Vita e della Sostenibilità Ambientale, University of Parma, Parco Area delle Scienze 17/A, 43124 Parma, Italy and [b]CIRCMSB (Consorzio Interuniversitario di Ricerca in Chimica dei Metalli nei Sistemi Biologici), Parma Unit, University of Parma, Italy, [c]Dipartimento di Scienze degli Alimenti e del Farmaco, University of Parma, Parco Area delle Scienze 27/A, 43124 Parma, Italy, [d]Dipartimento di Chimica e Farmacia, Università di Sassari, Via Vienna 2, I-07100 Sassari, Italy, [e]Rega Institute for Medical Research, KU Leuven – University of Leuven, B-3000 Leuven, Belgium

*Corresponding author:

email: mauro.carcelli@unipr.it
Dipartimento di Scienze Chimiche, della Vita e della Sostenibilità Ambientale
Università di Parma
Phone: +39 0521 905427
Fax: +39 0521 905557

Abstract

Influenza virus is an hot topic in medicinal chemistry and great efforts are ongoing for the discover of new antivirals able to overcome problems related to resistant strains and adverse side effects of current drugs. Influenza virus endonuclease is an attractive target for antiviral drug development and in particular the strategy to chelate the metal ion(s) within the active site proved to be an efficient mode to inhibit enzymatic activity. Our previous findings revealed that 2-hydroxyamide derivatives are able to chelate Mg^{2+} ions, forming complexes with different stoichiometric ratios. Here we report on the activity of the three ligands *N*-(4-fluorobenzyl)-2-hydroxybenzamide, *N*-(4-fluorobenzyl)-2,3-dihydroxybenzamide, and *N1,N3*-bis(4-fluorobenzyl)-2-hydroxyisophthalamide, containing the salicylic group, and their Mg^{2+} complexes **(7)-(9)**, evaluated by means of virus yield assay in influenza virus-infected MDCK cells and vRNP reconstitution assay in HEK293T cells. In some cases, promising anti-influenza activity with EC_{50} values in the low micromolar range were found. As a contribute to clarify the activity in cells of the ligands, here we also present a study on the their coordinating properties towards the other essential metal ion Cu(II), carried out by potentiometric and calorimetric measurements.

Keywords: chelating ligands; magnesium complexes; ITC measurements; influenza virus endonuclease; antiviral activity.

1. Introduction

Influenza virus is an enveloped virus with a segmented negative-oriented single-stranded RNA genome, belonging to the *Orthomyxoviridae*.[1] Seasonal human influenza A or B virus infections are an important cause of morbidity and mortality;[2] moreover there is a permanent risk of sudden influenza pandemics, such as the notorious 'Spanish flu' in 1918[3] and the swine-origin H1N1 pandemic in 2009.[4] Influenza vaccination is a widely used prophylactic measure, whereas two classes of anti-influenza

virus drugs are available, acting on the viral M2 ion-channel (amantadine and rimantadine) or the viral neuraminidase (zanamivir and oseltamivir). The M2 inhibitors have limited clinical utility due to their central nervous system side effects, in addition resistance is a growing concern for both M2 inhibitors and oseltamivir.[5,6,7,8,9] Therefore, there is an urgent need for new antiviral compounds, preferably based upon novel pharmacophores and different modes of action.[10]

The influenza virus polymerase is widely recognized as an attractive target for antiviral drug development: inhibition of its PA endonuclease, in particular, has deserved much attention in recent years.[11,12,13] The influenza virus polymerase complex is composed of three subunits: PB1, PB2 and PA.[14,15] The endonuclease catalytic site resides in the N-terminal domain of PA (PA-Nter).[16,17,18] The number and type of ions present in the catalytic site are not definitely clarified: it seems to contain one,[17,19] two,[16,20] or even three[21] manganese(II) or, more probably,[22,23] magnesium(II) ions as metal cofactors. Anyway, the two-metal-ion model is supported by several biochemical findings.[24,25] Diverse PA-binding agents with metal-chelating properties have been identified as influenza endonuclease inhibitors (**Figure 1**): 2,4-dioxobutanoic acid derivatives,[26,27] flutimide and its derivatives,[28] tetramic acids,[29] 5-hydroxypyrimidin-4-one derivatives,[30] marchantins[31] and green tea catechins, like epigallocatechin-3-gallate.[32,33] These inhibitors share a common pharmacophoric motif that is likely responsible for sequestration of the metal ions in the catalytic site of PA-Nter.

In recent years, we focused our research on chemical scaffolds that are able to chelate the metal ions in the PA-Nter active site, resulting in inhibition of influenza PA endonuclease activity.[34,35,36] More specifically, considering the functional resemblance between the active sites of HIV integrase and PA-Nter,[12] we focused here our attention on *N*-(4-fluorobenzyl)-2-hydroxybenzamide, *N*-(4-fluorobenzyl)-2,3-dihydroxybenzamide, and *N1,N3*-bis(4-fluorobenzyl)-2-hydroxyisophthalamide (**HL^1**, **H_2L^2**, and **HL^3, Scheme 1**), previously tested as HIV integrase inhibitors,[37] and containing the salicylic group.

These molecules have different coordinating abilities (**Figure 2**); in particular, **HL^1**, **H_2L^2**, and **HL^3** are able to chelate Mg^{2+} ions, forming complexes with different stoichiometric ratios (**Scheme 1**).[34]

Here we report on the activity of **HL^1**-**HL^3** and the Mg^{2+} complexes **(7)**-**(9)**, evaluated by means of virus yield assay in influenza virus-infected MDCK cells and vRNP reconstitution assay in HEK293T cells. Even if it is premature to advance hypothesis about the mechanism of action of these compounds in cells, it seemed reasonably to connect the activity of **HL^1**-**HL^3** also to their possibility to chelate the metal ions in the PA-Nter active site. The importance to advance in the understanding of the coordination chemistry of **HL^1**-**HL^3**, move us to investigate also their chemistry in solution with copper(II) ion, another essential trace element.

2. Experimental

2.1 Chemistry. All reagents of commercial quality were used without further purification. Purity of compounds was determined by elemental analysis and verified to be ≥95% for all synthesized molecules. NMR spectra were recorded at 25 °C on a Bruker Avance 400 FT spectrophotometer. The ATR-IR spectra were recorded by means of a Nicolet-Nexus (Thermo Fisher) spectrophotometer by using a diamond crystal plate in the range of 4000-400 cm^{-1}. Elemental analyses were performed by using a FlashEA 1112 series CHNS/O analyzer (Thermo Fisher) with gas-chromatographic separation. Electrospray mass spectral analyses (ESI-MS) were performed with an electrospray ionization (ESI) time-of-flight Micromass 4LCZ spectrometer. MS spectra were acquired in positive EI mode by means of a DEP-probe (Direct Exposure Probe) mounting on the tip a Re-filament with a DSQII Thermo Fisher apparatus, equipped with a single quadrupole analyzer. **HL^1**, **H_2L^2** and **HL^3** and the corresponding magnesium complexes **7-9** were synthesized according to slightly modified literature procedures[34] (see Supporting information for the chemical characterization).

2.2 Potentiometric titrations. The Cu(II) stock solutions were prepared from $CuCl_2 \cdot 2H_2O$ (Merck) and bidistilled water and were acidified by adding HCl to avoid Cu(II) hydrolysis. The concentration of the excess H^+ was obtained by titrating with KOH. Cu(II) concentration was determined by using

EDTA as a titrant in the presence of concentrated ammonia using Fast Sulfon Black as indicator. Equilibrium constants for protonation and complexation were determined by means of potentiometric titrations in methanol:water=9:1 v/v solution at ionic strength of 0.1 M KCl. The titrations were carried out under nitrogen in the pH range 2.5-11 by using a fully automated apparatus equipped with a CRISON GLP 21-22 digital voltmeter (resolution 0.1 mV) and a 5 ml Metrohm Dosimat 655 autoburet, and controlled by a homemade software. Temperature (25 ± 0.1 °C) was controlled to ± 0.1°C by using a thermostatic circulating water bath (ISCOGTR 2000 IIx). The electrodic chain (Crison 5250 glass electrode and 0.1 M KCl in methanol:water = 9:1 v/v calomel electrode, Radiometer 401) was calibrated in terms of $[H^+]$ by means of a strong acid – strong base titration by Gran's method[38] allowing for the determination of the standard potential, E° (371.5 ± 0.4 mV), and of the ionic product of water, K_w (pK_w = 14.40 ± 0.05). Appropriate aliquots of ligand solution, prepared by weight, were titrated with standard KOH (methanol:water = 9:1 v/v, I = 0.1 M KCl) with and without metal ions, applying constant speed magnetic stirring. Freshly boiled methanol and double-distilled water, kept under nitrogen, were used throughout. The experimental procedure to reach high accuracy in the determination of the equilibrium constants in this mixed solvent has been described in detail elsewhere.[39] The protonation constants of **HL**[1], **H_2L**[2] and **HL**[3] were obtained by titrating 20 ml of samples of each ligand (3×10^{-3} M). For obtaining the complex formation constants, titrations were performed in different ligand/metal ratios (from 1 up to 4). At least two measurements (about 60 experimental points each) were performed for each system. The software HYPERQUAD[40] was used for obtaining the speciation and the logarithm of the stability constants ($\log \beta_{pqr}$) from titration data. $\beta_{pqr} = [M_pL_qH_r]/[M]^p[L]^q[H]^r$ is the cumulative formation constant for the equilibrium reaction $pM + qL + rH = M_pL_qH_r$, in which M indicates the metal, L the completely deprotonated ligand and H the proton. Charges are omitted for simplicity.

2.3 Isothermal titration calorimetry (ITC). ITC measurements were carried out on a CSC model 5300 N-ITC III isothermal titration calorimeter (Calorimetry Sciences Corporations, USA) at 25°C.

KOH solution (0.065–0.145 M) in methanol:water = 9:1 at 0.1 M KCl ionic strength was injected in steps of 5 μL into a 960 μL reaction cell by a 250 μL syringe with an interval of 400-500 s between two successive injections, with stirring speed of 150 revolutions per minute (rpm), following the procedure previously described.[41] For obtaining the protonation heat of the ligand, the cell was filled up with a solution of the ligand in methanol:water = 9:1, 0.1 M KCl ionic strength. Dilution heats were subtracted by carrying out blank experiments, in which the KOH solution was injected into the same solvent, without ligand. The molar enthalpy change for the reaction $H^+ + OH^- = H_2O$ was obtained by titrating a solution of HCl (in the cell) by KOH, in the burette, both prepared in methanol:water = 9:1 at ionic strength 0.1 M KCl. It results -20.6±0.4 kJ mol^{-1}.[41] The experimental peaks were integrated and corrected for the dilution heats by the NanoAnalyze (TA Instrument) software. The data so obtained were elaborated by the HypΔH software,[41,42] assuming the protonation constants from potentiometric measurements.

2.4 Cells and media. Madin-Darby canine kidney (MDCK) cells (a kind gift from Dr. M. Matrosovich, Marburg, Germany) and human embryonic kidney 293T (HEK293T) cells (purchased from Thermo Fisher Scientific, Waltham, MA) were cultivated in Dulbecco's modified Eagle medium supplemented with 10% fetal calf serum, 1 mM sodium pyruvate, and 0.075% sodium bicarbonate. During virus experiments, the MDCK cells were maintained in MDCK infection medium, consisting of Ultra MDCK medium (Lonza, Basel, Switzerland) supplemented with 0.0225% sodium bicarbonate, 2 mM L-glutamine, and 2 μg/ml tosyl phenylalanyl chloromethyl keton (TPCK) - treated trypsin (Sigma-Aldrich, St. Louis, MO). Cells were incubated in a humidified atmosphere containing 5% CO_2.

2.5 vRNP reconstitution assay. The procedure to determine the inhibitory effect of the compounds on influenza vRNPs reconstituted in HEK293T cells, is described in full detail elsewhere.[43] Briefly, the four relevant plasmids (i.e. the expression plasmids for PB1, PB2, PA and NP) were combined with the firefly luciferase reporter plasmid, and co-transfected into HEK293T cells using Lipofectamin 2000

(Invitrogen, Life Technologies, Gent, Belgium). After incubation at 37°C for 24 h in the presence of serial dilutions of the test compounds, the ONE-Glo luciferase assay system (Promega, Madison, WI) was used to determine luciferase activity. The 50% effective concentration (EC_{50}) was defined as the compound concentration causing 50% reduction in the vRNP-driven luciferase signal, as compared to cells receiving medium instead of compound. These EC_{50} values were calculated by non-linear regression analysis using GraphPad Prism software, on data from 2-5 experiments. In parallel, compound cytotoxic activity was determined in untransfected HEK293T cells which had been incubated with serial dilutions of the compounds for 24 h, using the MTS cell viability assay (CellTiter 96 AQ_{ueous} One Solution Cell Proliferation Assay, Promega). These spectrophotometric data were used to calculate the 50% cytotoxic concentration (CC_{50}), i.e. the concentration reducing cell viability by 50%, as compared to wells receiving medium instead of compound. Ribavirin (Virazole; ICN Pharmaceuticals, Costa Mesa, CA) was included as the reference compound.

2.6 Virus yield assay. We previously published in full detail the virus yield assay to determine the anti-influenza virus activity in MDCK cell cultures. [44] Briefly, one day prior to infection, MDCK cells were seeded into 96-well plates at 25,000 cells per well. At day 0, serial dilutions of the test compounds were added, immediately followed by infection with influenza A/PR/8/34 virus. After 24 h incubation at 35°C, the virus amount in the supernatants was estimated by determining the viral genome copy number in a one-step quantitative real-time reverse transcription (qRT)-PCR assay (CellsDirect One-Step qRT-PCR kit; Invitrogen), with influenza virus M1-specific primers and probe. The EC_{99} and EC_{90} values were calculated by interpolation from data of 2-3 experiments, and defined as the compound concentration causing respectively a 2-$\log_{10}$ and 1-$\log_{10}$ reduction in viral RNA (vRNA) copy number, as compared to the virus control receiving no compound. In parallel, the CC_{50} values after 24 h incubation with compounds were determined in uninfected MDCK cells, using the spectrophotometric MTS cell viability assay described above, respectively. Ribavirin was included as the reference compound.

3. Results and Discussion

Salicylamides **(1)-(3)** were obtained with good yields (**Scheme 1**);[34] deprotection of the hydroxyl groups was then carried out with 1M solution of boron tribromide to obtain $\mathbf{HL^1}$, $\mathbf{H_2L^2}$ and $\mathbf{HL^3}$ (**Scheme 1**). The protonation constants of the salicylic OH are 9.51(1) for $\mathbf{HL^1}$, 9.11(1) for $\mathbf{H_2L^2}$, and 7.28(1) for $\mathbf{HL^3}$; the second acidity constant for $\mathbf{H_2L^2}$ is greater than 12, out of the working range of the glass electrode.[34] The thermodynamic study of the protonation of the ligands was completed by performing ITC experiments and the results are shown in **Table 1**; in **Figure 3** the comparison between experimental and computed cumulative heats for $\mathbf{HL^1}$ are reported (data for $\mathbf{H_2L^2}$ and $\mathbf{HL^3}$ are in Supporting information). The complexes $Mg(L^1)_2{\cdot}3H_2O$ **(7)**, $Mg_2(L^2)_2{\cdot}2.5H_2O$ **(8)** and $Mg(L^3)_2{\cdot}3H_2O$ **(9)** (**Scheme 1**) were synthesized and characterized (see Supporting information) as previously disclosed.[34] We want to evaluate the activity of $\mathbf{HL^1}$, $\mathbf{H_2L}$, and $\mathbf{HL^3}$ in influenza virus-infected cells. In the cell the ligands $\mathbf{HL^1}$, $\mathbf{H_2L}$, and $\mathbf{HL^3}$ could interact with ions different from the Mg(II) of the active site of PA-Nter, so their coordinating properties towards copper(II), another essential trace element, are also investigated for comparison. As far as the potentiometric titrations of the ligand/Cu(II) systems are concerned, we had to deal with poor solubility in the systems $\mathbf{HL^1}$/Cu(II) and $\mathbf{HL^3}$/Cu(II). In particular, for $\mathbf{HL^1}$ we found the presence of a precipitate in the pH range 6 – 8 for metal:ligand *ratio* 1:2 and around pH = 6 for the metal:ligand *ratio* 1:4. We suppose that the species $Cu\mathbf{HL^1}$ is poorly soluble. The precipitate is formed above pH 8 (1:4 *ratio*) and above pH 9 (1:2 *ratio*) with $\mathbf{HL^3}$, probably due the formation of insoluble hydroxylated species**.** Only the experimental points in which the solution appeared clear were processed by the software HYPERQUAD[40]. The models of speciation in solution for the ligands and Cu(II), showing the best statistical parameters and the best fit between experimental and computed potentiometric titration curves, are shown in **Table 2**. The distribution diagrams as a function of the pH, evaluated for metal to ligand *ratio* 4:1, [Cu(II)] = 25

mM, are reported in **Figure 4**. As expected, the ligands have a greater affinity towards Cu(II) than towards Mg(II) (see Supporting information for the distribution diagrams and the formation constants with Mg(II)).[34] This can give rise to some doubts regarding the stability of the Mg(II) complexes (**7**)-(**9**) in cells, even if, obviously, Cu(II) is not uncoordinated in cells and the resulting equilibria are more complex. While Mg(II) starts to bind the ligand at a pH value at which it is already deprotonated, probably forming outer sphere complexes, Cu(II) is able to lower the pK_a value of the ligand of a few units, forming complex species already at acidic pH. **HL^1** and **HL^3** give rise to the same species in solution, namely CuL, CuL_2 and CuL_2H_{-1}, with similar affinity. In the case of **HL^1**, the precipitate formed around pH = 7 could be the neutral specie CuL_2, that then re-solubilizes forming CuL_2H_{-1}. Moreover, for **HL^1** we were able to find out also the species CuL_2H_{-2}, formed beyond pH = 10 and probably due to the dissociation of two water molecules completing the coordination sphere of the Cu(II) ion. It was not possible to search for this species in the case of **HL^3**, because the solution is turning opaque beyond pH = 9, probably due to the precipitation of hydroxylated compounds. **H_2L^2** gives rise to the same species as **HL^1**, but seems unable to form the complex CuL_2. At physiological pH the species CuL_2 is the most abundant for **HL^3**, it reaches only a few percent for **HL^1** and it is completely absent for **H_2L^2**. These last two ligands at neutral pH form preferably the species ML. We have also examined the hypothesis of the formation in solution of di-metallic species M_2L_2, but they were always rejected by the software.

3.1 Anti-influenza virus activity in enzymatic and cellular assays. The hydroxybenzamide-based ligands **HL^1-HL^3** and their magnesium(II) complexes (**7**)-(**9**) were previously tested for their ability to inhibit the PA endonuclease activity in an enzymatic assay with recombinant PA-Nter (**Table 3**):[34] **(8)** proved to be the most active compound, with an IC_{50} of 18 µM, which is 3-fold higher than that of the reference compound DPBA, but lower than the value of the corresponding free ligand **H_2L^2** (IC_{50} = 33 µM). On the contrary, **HL^1, HL^3** and the complexes **(7)** and **(9)** did not inhibit the endonuclease reaction at 500 µM, the highest concentration tested. These results of the enzymatic assays, moved us

now to evaluate these compounds in two cellular assays, a reporter-based vRNP reconstitution assay in HEK293T cells and a virus yield assay in MDCK cells (**Table 3**). In the vRNP reconstitution assay, which is well suited to determine the activity and selectivity of possible PA endonuclease inhibitors in cell culture, the effect of the compounds on the activity of reconstituted vRNPs is measured. **HL^3** and the corresponding complex **(9)** displayed the most potent antiviral activity, with EC_{50} values of 6.7 and 3.1 µM respectively (**Table 3**), and a selectivity index (ratio of CC_{50} to EC_{50}) of 10. In the virus yield assay on the other hand, the magnesium complexes showed the best antiviral profile, with EC_{90} values of 81, 87 and 8.5 µM for **(7)**, **(8)** and **(9)**, respectively.

Comparison of the biological activities reported in **Table 3** shows for some compounds a discrepancy between anti-influenza virus activity in cells and inhibition in the PA-Nter enzymatic assay. This is an indication that these compounds probably act also on a PA-unrelated target in virus-infected cell cultures. Their antiviral activity could be related to inhibition of influenza virus entry, viral RNA synthesis, or a stage beyond viral RNA synthesis (possibly virus maturation or release). In order to clearly define the antiviral target of these different molecules, specific mechanistic experiments are currently ongoing.

4.1 CONCLUSIONS

Salicylamides have been studied for their biological properties for a long time.[45] In the present work we show that salicylamides **HL^1**-**HL^3** and their Mg(II) complexes (**7**)-(**9**) have interesting activity against influenza virus in cells. It is worth of note that, in some cases, the best antiviral profiles are shown by the metal complexes. Even in these cases, however, it is difficult to know if the complexes are the effective drug or, more properly, pro-drugs. In the biological medium, in fact, there are metal ions and ligands that can behave as competitors. The complexing properties of the salicylamides in solution suggested that their activity can be due to the possibility to chelate the Mg(II) ions in the active site of influenza virus

endonuclease. However, the copper(II) complexes of **HL[1]**-**HL[3]** are more stable than the corresponding magnesium(II) ones: in cells free copper(II) is present at low concentrations, but it is difficult to think that **HL[1]**-**HL[3]** can act as uncomplexed ligands. On the other side, in cells the magnesium(II) complexes (**7**)-(**9**) could give rise to transmetallation. In conclusion, care has to be taken in the individuation of the chemical species responsible for the biological activity. Another, possibly correlated, notable point to be considered is that some compounds (**HL[1]** or **HL[3]**, for example) are more active in cells than in the enzyme assays. Analysis of the (multitarget?) mechanism of action and full pharmocological properties of similar salicylamides and their metal complexes are warranted in follow-up studies.

Abbreviations

CC_{50}	50% cytotoxic concentration
DEP	Direct Exposure Probe
DPBA	2,4-dioxo-4-phenylbutanoic acid
$EC_{50,}$ $EC_{90,}$ EC_{99}	50%, 90%, 99% maximal effective concentration
ESI-MS	Electrospray mass spectral analyses
HEK293T cells	human embryonic kidney 293T cells
ITC	Isothermal Titration Calorimetry
MDCK cells	Madin-Darby canine kidney cells
PA-Nter	N-terminal domain of PA
vRNPs	viral ribonucleoproteins

Author Contributions

The manuscript was written through contributions of all authors. All authors have given approval to the final version of the manuscript.

ACKNOWLEDGMENTS

"Centro Interdipartimentale Misure Giuseppe Casnati" of the University of Parma are thanked for facilities.

Table 1. Thermodynamic parameters for the protonation of the ligands under study. In brackets the standard deviation on the last figure.

	logK_a	ΔG (kJ mol^{-1})	ΔH (kJ mol^{-1})	ΔS (J K^{-1}mol^{-1})
HL[1]	9.51(1)	-54.27(2)	-10.9(1)	145(2)
H_2L[2]	9.11(1)	-51.99(2)	-16.9(5)	117(4)
HL[3]	7.28(1)	-41.54(2)	-8.6(2)	110(2)

Table 2. Logarithms of the formation constants ($\beta_{pqr} = [M_pL_qH_r]/[M]^p[L]^q[H]^r$) in methanol:water = 9:1 v/v, I = 0.1 M KCl at 25 °C for the ligands under study with Cu(II). SDs are given in parentheses.

p	q	r	HL^1	H_2L^2	HL^3
1	1	0	5.66(37)	8.74(6)	5.42(6)
1	2	0	8.99(47)		9.22(10)
1	2	-1	0.10(38)	4.53(7)	0.82(8)
1	2	-2	-12.02(38)	-6.70(11)	

Table 3. Inhibitory activity of ligands **HL[1]-HL[3]** and Mg^{2+} complexes **(7)-(9)** in the enzymatic assay with influenza virus PA-Nter endonuclease,[34] or in cellular influenza virus assays based on virus yield or vRNP reconstitution.

Compound	Enzyme assay with PA-Nter[a]	Virus yield assay in influenza virus-infected MDCK cells[b]				vRNP reconstitution assay in HEK293T cells[c]	
		Antiviral Activity		Cytotoxicity		Activity	Cytotoxicity
	IC_{50}	EC_{99}	EC_{90}	MCC	CC_{50}	EC_{50}	CC_{50}
HL[1]	>500	>200	>200	>200	148	35	155
H_2L^2	33	>50	>50	50	>180	20	79
HL[3]	>500	>200	>200	>200	>144	6.7	74
(7)	>500	126	81	•200	>151	104	>200
(8)	18	•125	87	113	>194	24	44
(9)	>500	13	8.5	50	41	3.1	30
DPBA[d]	5.5	-	-	-	-	-	-
Ribavirin	-	13	8.5	•200	>200	9.3	>200

[a]Published results in the enzymatic PA-Nter endonuclease assay.[34]

[b]MDCK (Madin-Darby canine kidney) cells were infected with influenza A virus (strain A/PR/8/34) and incubated with the compounds during 24 h. The virus yield in the supernatant was assessed by real-time qPCR. The EC_{99} and EC_{90} values represent the compound concentrations (in µM) producing a 2-log10 or 1-log10 reduction in virus titer, respectively. The cytotoxicity, assessed in uninfected MDCK cells, was expressed as the CC_{50} value (50% cytotoxic concentration, determined with the MTS cell viability assay, in µM).

[c]HEK293T (human embryonic kidney 293T) cells were co-transfected with the four vRNP-reconstituting plasmids and the luciferase reporter plasmid in the presence of the test compounds. The EC_{50} value represents the compound concentration (in µM) producing 50% reduction in vRNP-driven firefly reporter signal, estimated at 24 h after transfection. The CC_{50} (in µM), i.e. the 50% cytotoxic concentration, was determined in untransfected HEK293T cells by MTS cell viability assay.

[d]DPBA, 2,4-dioxo-4-phenylbutanoic acid, used as reference.

References

[1] Lamb, R. A.; Krug, R. M. Orthomyxoviridae: the viruses and their replication. In *Fields virology*, *4th ed.* (Eds. Knipe, D. M., Howley, P. M., Griffin, D. E., Lamb, R. A., Martin, M. A., Roizman, B., Straus, S. E.) 1487-1531 (Lippincott Williams & Wilkins: Philadelphia, 2001).

[2] World Health Organization. Influenza (seasonal)-Fact sheet N°211. http://www.who.int/mediacentre/factsheets/fs211/en/ (accessed 19-1-2015).

[3] Taubenberger, J. K.; Morens, D. M. 1918 Influenza: the mother of all pandemics. *Emerg. Infect. Dis.* **12**, 15-22 (2006).

[4] Garten, R. J.; Davis, C. T.; Russell, C. A.; Shu, B.; Lindstrom, S. et al. Antigenic and genetic characteristics of swine-origin 2009 A(H1N1) influenza viruses circulating in humans. *Science*, **325**, 197–201 (2009).

[5] Jefferson, T.; Demicheli, V.; Di Pietrantonj, C.; Rivetti, D. Amantadine and rimantadine for influenza A in adults. Cochrane Database. *Syst. Rev.* CD001169 (2006).

[6] Deyde, V. M.; Xu, X.; Bright, R. A.; Shaw, M.; Smith, C. B. et al. Surveillance of resistance to adamantanes among influenza A(H3N2) and A(H1N1) viruses isolated worldwide. *J. Infect. Dis.* **196**, 249-257 (2007).

[7] Moscona, A. Global transmission of oseltamivir-resistant influenza. *N. Engl. J. Med.* **360**, 953-956 (2009).

[8] Memoli, M.J.; Davis, A.S.; Proudfoot, K.; Chertow, D.S.; Hrabal, R.J et al. Multidrug-resistant 2009 pandemic influenza A(H1N1) viruses maintain fitness and transmissibility in ferrets. *J. Infect Dis.* **203**, 348–357 (2011).

[9] van der Vries, E.; Schutten, M.; Fraaij, P.; Boucher, C.; Osterhaus, A. Influenza virus resistance to antiviral therapy. *Adv. Pharmacol.* **67**, 217-246 (2013).

[10] Vanderlinden, E.; Naesens, L. Emerging antiviral strategies to interfere with influenza virus entry. *Med. Res. Rev.* **34**, 301–339 (2014).

[11] Yuan, S.; Chu, H.; Singh, K.; Zhao, H.; Zhang, K.; Kao, R. Y. T.; Chow, Billy K. C.; Zhou, J.; Zheng, B. A novel small-molecule inhibitor of influenza A virus acts by suppressing PA endonuclease activity of the viral polymerase. *Scientific Reports* **6**, 22880 (2016).

[12] Rogolino, D.; Carcelli, M.; Sechi, M.; Neamati, N. Viral enzymes containing magnesium: metal binding as a successful strategy in drug design. *Coord. Chem. Rev.* **256**, 3063-3086 (2012).

[13] Stevaert, A.; Naesens, L. The Influenza Virus Polymerase Complex: An Update on Its Structure, Functions, and Significance for Antiviral Drug Design. *Med Res Rev*. **36**, 1127-1173 (2016).

[14] Pflug, A.; Guilligay, D.; Reich, S.; Cusack, S. Structure of influenza A polymerase bound to the viral RNA promoter. *Nature* **516**, 355-360 (2014).

[15] Velthuis, A.; Fodor, E. Influenza virus RNA polymerase: insights into the mechanisms of viral RNA synthesis. *Nature Rev. Microbiol.* **14**, 479–493 (2016).

[16] Dias, A.; Bouvier, D.; Crépin, T.; McCarthy, A. A.; Hart, D. J. et al. The cap-snatching endonuclease of influenza virus polymerase resides in the PA subunit. *Nature* **458**, 914-918 (2009).

[17] Yuan, P.; Bartlam, M.; Lou, Z.; Chen, S.; Zhou, J. et al. Crystal structure of an avian influenza polymerase PA(N) reveals an endonuclease active site. *Nature* **458**, 909-913 (2009).

[18] Tefsen, B.; Lu, G.; Zhu, Y.; Haywood, J.; Zhao, L. et al. The N-terminal domain of PA from bat-derived influenza-like virus H17N10 has endonuclease activity. *J. Virol.* **88**, 1935-1941 (2014).

[19] Zhao, C.; Lou, Z.; Guo, Y.; Ma, M.; Chen, Y. et al. Nucleoside monophosphate complex structures of the endonuclease domain from the influenza virus polymerase PA subunit reveal the substrate binding site inside the catalytic center. *J. Virol.* **83**, 9024-9030 (2009).

[20] DuBois, R. M.; Slavish, P. J.; Baughman, B. M.; Yun, M. K.; Bao, J. et al. Structural and biochemical basis for development of influenza virus inhibitors targeting the PA endonuclease. *PLoS Pathog.* **8**, e1002830 (2012).

[21] Bauman, J. D.; Patel, D.; Baker, S. F.; Vijayan, R. S.; Xiang, A. et al. Crystallographic fragment screening and structure-based optimization yields a new class of influenza endonuclease inhibitors. *ACS Chem. Biol.* **8**, 2501-2508 (2013).

[22] Maret, W. Metalloproteomics, metalloproteomes, and the annotation of metalloproteins. *Metallomics* **2**, 117-125 (2010).

[23] Jahnen-Dechent, W.; Ketteler, M. Magnesium basics. *Clin. Kidney J.*, **5**, i3-i14 (2012).

[24] Doan, L.; Handa, B.; Roberts, N. A.; Klumpp, K. Metal ion catalysis of RNA cleavage by the influenza virus endonuclease. *Biochemistry* **38**, 5612-5619 (1999).

25 Crépin T1, Dias A, Palencia A, Swale C, Cusack S, Ruigrok RW. Mutational and metal binding analysis of the endonuclease domain of the influenza virus polymerase PA subunit. *J Virol.* **84**, 9096-104 (2010).

26 Hastings, J. C.; Selnick, H.; Wolanski, B.; Tomassini, J. E. Anti-influenza virus activities of 4-substituted 2,4-dioxobutanoic acid inhibitors. Antimicrob. Agents Chemother. **40**, 1304-1307 (1996).

[27] Stevaert, A.; Nurra, S.; Pala, N.; Carcelli, M.; Rogolino, D. et al. An integrated biological approach to guide the development of metal-chelating inhibitors of influenza virus PA endonuclease. *Mol. Pharmacol.* **87**, 323-337 (2015).

[28] Tomassini, J. E.; Davies, M. E.; Hastings, J. C.; Lingham, R.; Mojena, M. et al. A novel antiviral agent which inhibits the endonuclease of influenza viruses. *Antimicrob. Agents Chemother.* **40**, 1189-1193 (1996).

[29] Parkes, K. E.; Ermert, P.; Fässler, J.; Ives, J.; Martin, J. A.; Merrett, J. H.; Obrecht, D.; Williams, G.; Klumpp, K. Use of a pharmacophore model to discover a new class of influenza endonuclease inhibitors. *J. Med. Chem.* **46**, 1153-1164 (2003).

[30] Sagong, H. Y.; Bauman, J. D.; Patel, D.; Das, K.; Arnold, E.; Lavoie, E. J. Phenyl substituted 4-hydroxypyridazin-3(2*H*)-ones and 5-hydroxypyrimidin-4(3*H*)-ones: inhibitors of influenza A endonuclease. *J. Med. Chem.* **57**, 8086-8098 (2014).

[31] Iwai, Y.; Murakami, K.; Gomi, Y.; Hashimoto, T.; Asakawa, Y. et al. Anti-influenza activity of marchantins, macrocyclic bisbibenzyls contained in liverworts. *PLoS One* **6**, e19825 (2011).

[32] Kuzuhara, T.; Iwai, Y.; Takahashi, H.; Hatakeyama, D.; Echigo, N. Green tea catechins inhibit the endonuclease activity of influenza A virus RNA polymerase. *PLoS Curr.* **1**, RRN1052 (2009).

[33] Song, J. M.; Lee, K. H.; Seong, B. L. Antiviral effect of catechins in green tea on influenza virus. *Antiviral Res.* **68**, 66–74 (2005).

[34] Carcelli, M.; Rogolino, D.; Bacchi, A.; Rispoli, G.; Fisicaro, E. et al. Metal-chelating 2-hydroxyphenyl amide pharmacophore for inhibition of influenza virus endonuclease. *Mol. Pharmaceutics* **11**, 304-316 (2014).

[35] Rogolino, D.; Bacchi, A.; De Luca, L.; Rispoli, G.; Sechi M. et al. Investigation of the salicylaldehyde thiosemicarbazone scaffold for inhibition of influenza virus PA endonuclease. *J. Biol. Inorg. Chem.* **20**, 1109-1121 (2015).

[36] Carcelli, M.; Rogolino, D.; Gatti, A.; De Luca, L.; Sechi, M.; Kumar, G.; White, S.; Stevaert, A.; Naesens, L. N-acylhydrazone inhibitors of influenza virus PA endonuclease with versatile metal binding modes. *Scientific Reports* **6**, 31500 (2016).

[37] Agrawal, A.; DeSoto, J.; Fullagar, J. L.; Maddali, K.; Rostami, S.; Richman, D. D.; Pommier, Y.; Cohen, S. M. Probing chelation motifs in HIV integrase inhibitors. *PNAS* **109**, 2251–2256 (2012).

[38] Gran, G. *Analyst* **77**, 661-671 (1952).

[39] Fisicaro, E.; Braibanti, A. Potentiometric titrations in methanol/water medium: intertitration variability, *Talanta* **10**, 769-774 (1988).

[40] Gans, P.; Sabatini, A.; Vacca, A. Investigation of equilibria in solution. Determination of equilibrium constants with HYPERQUAD suite of programs, *Talanta* **43**, 1739 (1996).

[41] Fisicaro, E.; Compari, C.; Bacciottini, F.; Contardi, L.; Carcelli, M.; Rispoli, G.; Rogolino, D., Thermodynamics of complexes formation by ITC in methanol/water = 9/1 (v/v) solution: A case study, *Thermochim. Acta* **586**, 40-44 (2014).

[42] Gans, A.; Sabatini, A.; Vacca, A. Simultaneous calculation of equilibrium constants and standard formation enthalpies from calorimetric data for systems with multiple equilibria in solution, *J. Solution Chem*. **37**, 467–476 (2008).

[43] Stevaert, A.; Dallocchio, R.; Dessì, A.; Pala, N.; Rogolino, D.; Sechi, M.; Naesens, L. Mutational analysis of the binding pockets of the diketo acid inhibitor L-742,001 in the influenza virus PA endonuclease. *J. Virol.* **87**, 10524-10538 (2013).

[44] Vanderlinden, E.; Göktas, F.; Cesur, Z.; Froeyen, M.; Reed, M. L.; Russell, C. J.; Cesur, N.; Naesens, L. Novel inhibitors of influenza virus fusion: structure-activity relationship and interaction with the viral hemagglutinin. *J. Virol.* **84**, 4277-4288 (2010**).**

[45] Krátký, M.; Vinšová, J. Antiviral activity of substituted salicylamides - a review. *Mini Rev. Med. Chem.* **11**, 956-967 (2011).

Scheme, Figure and Table captions

Scheme 1. Synthesis of the ligands **HL^1-HL^3** and the corresponding magnesium complexes **(7)-(9)**[a]

Figure 1. Some representative influenza endonuclease inhibitors with, in bold, their chelating chemotype.

Figure 2. One metal (**HL^1**) *versus* two metals binding (**H$_2$L^2** and **HL^3**) chelating modes.

Figure 3. a) Raw data from the ITC titration for the protonation of **HL^1**. Upward peaks indicate an exothermic reaction. Each peak corresponds to a single 5 µl injection. b) Comparison between experimental and computed cumulative heats (output from HypΔH software). Experimental conditions: **HL^1** 9.5 µmoles, titrant KOH 0.1 M.

Figure 4. Distribution diagrams for the systems ligand:Cu=2:1, [Cu^{2+}] = 1.25 mM. a) Ligand = **HL^1**, in the pH range 6-8 a precipitate is formed. b) Ligand = **H$_2$L^2**. c) Ligand = **HL^3**, the solution becomes cloudy above pH=9. The monodeprotonated ligands are indicated as L; charges are omitted for simplicity.

Table 1. Thermodynamic parameters for the protonation of the ligands under study. In brackets the standard deviation on the last figure.

Table 2. Logarithms of the formation constants ($\beta_{pqr} = [M_pL_qH_r]/[M]^p[L]^q[H]^r$) in methanol:water = 9:1 v/v, I = 0.1 M KCl at 25 °C for the ligands under study with Cu(II). SDs are given in parentheses.

Table 3. Inhibitory activity of ligands **HL^1-HL^3** and Mg^{2+} complexes **(7)-(9)** in the enzymatic assay with influenza virus PA-Nter endonuclease,[34] or in cellular influenza virus assays based on virus yield or vRNP reconstitution.

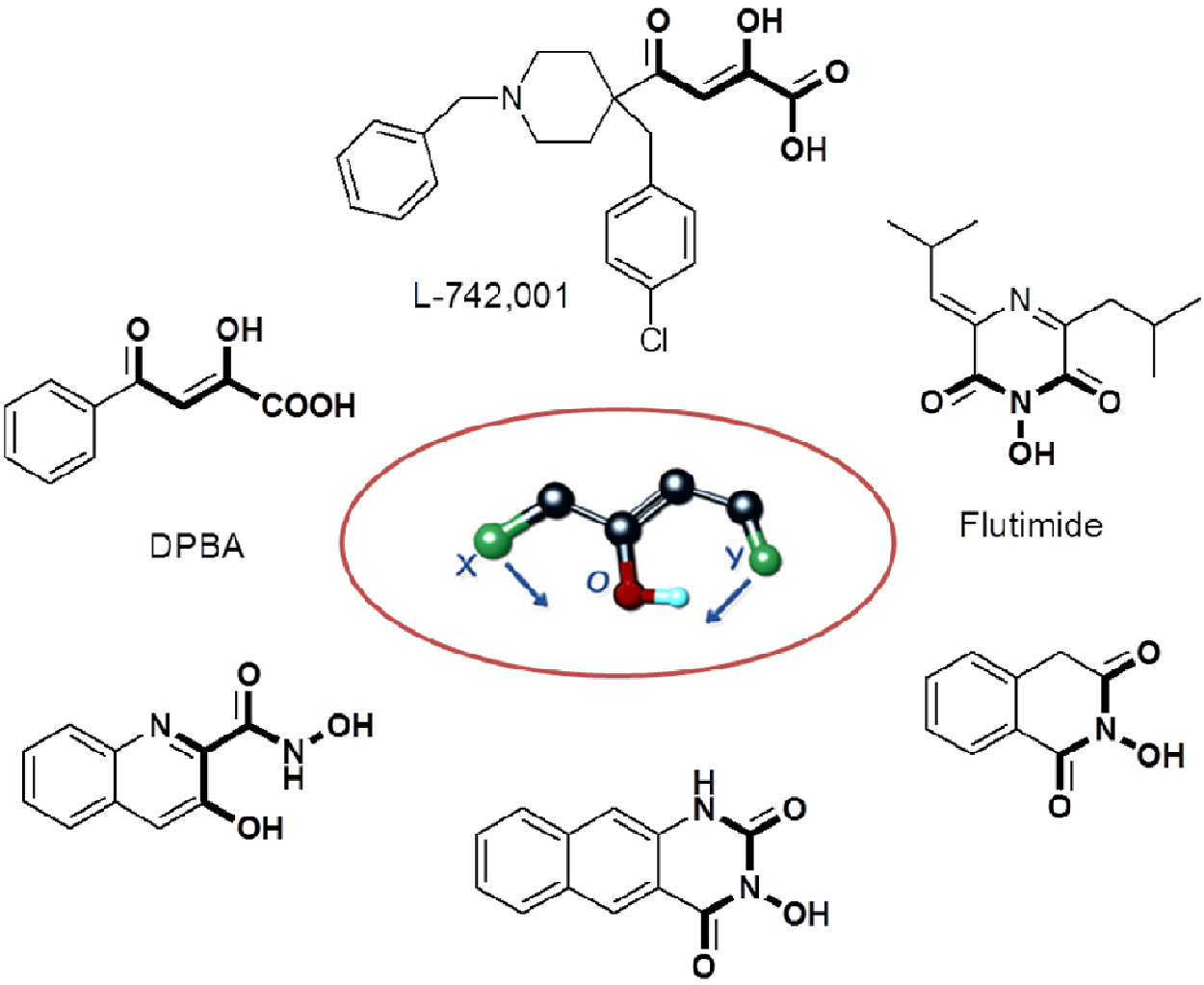

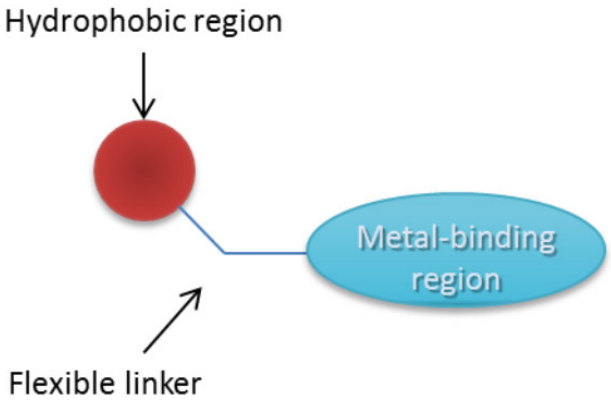

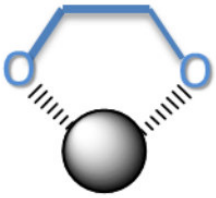

«one-metal» binding

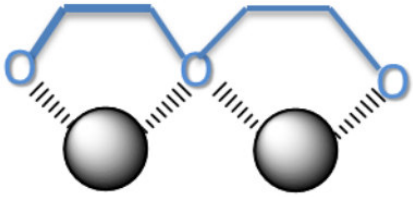

«two-metals» binding

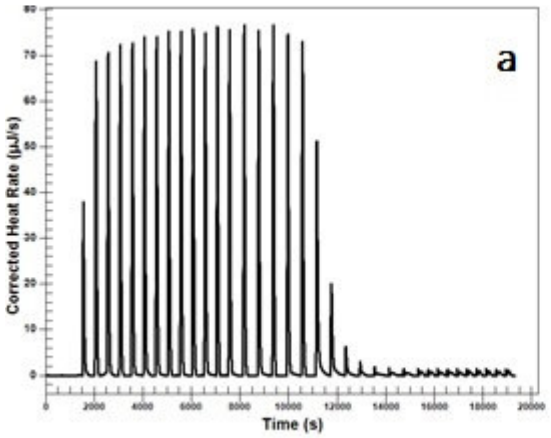

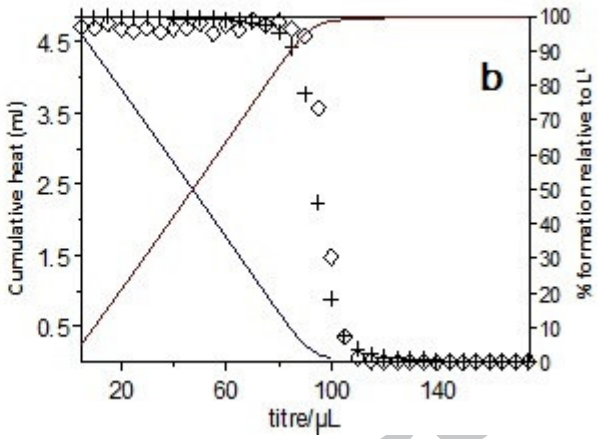

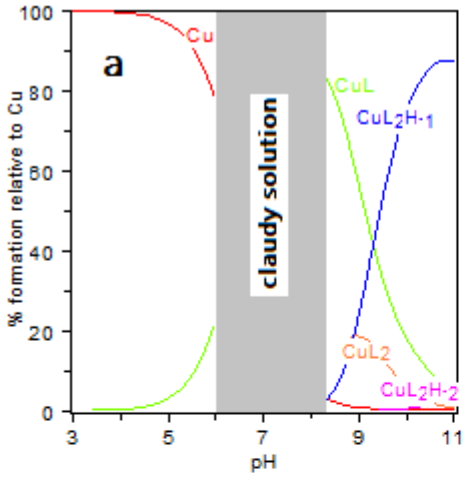

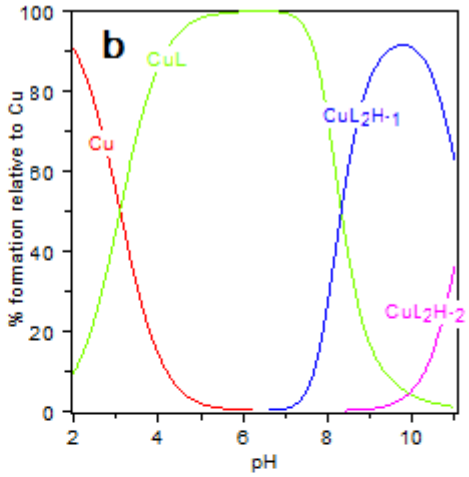

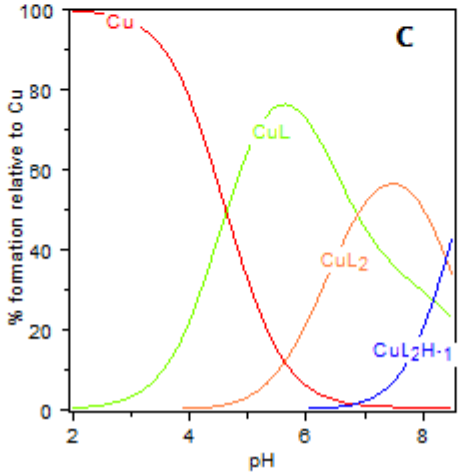

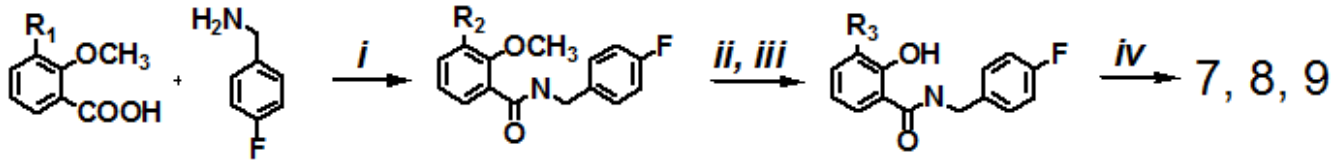

1: R_1 = H; R_2 = H
2: R_1 = OCH_3; R_2 = OCH_3
3: R_1 = COOH; R_2 = CONH*p*FBz

4, HL^1 : R_3 = H
5, H_2L^2 : R_3 = OH
6, HL^3 : R_3 = CONH*p*FBz

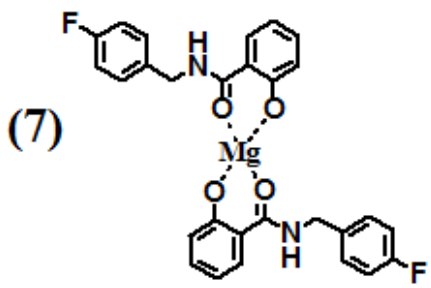

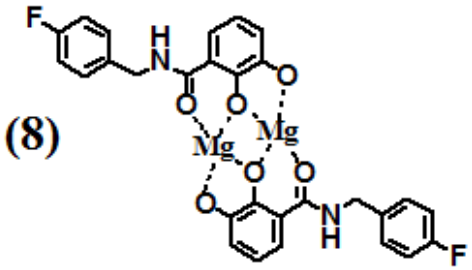

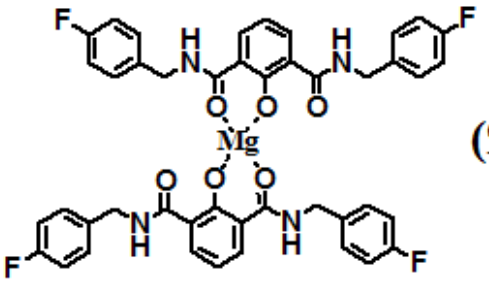

[a]Reagents and conditions: (i) carbonyldiimidazole, dichloromethane dry, r.t. 24 h. (ii) BI dichloromethane dry, T = 0°C to r.t., 24 h; (iii) NaOH 2M r.t. 30 min., methanol; (iv) $MgCl_2$ r.t. 5 h.

Graphical Abstract Synopsis

2-hydroxyamide pharmachophore can chelate metal cofactor(s) within influenza virus endonuclease. 2-Hydroxyamide ligands and their magnesium complexes have interesting antiviral activity on infected cells. However, investigation of solution behaviour of this pharmachophore highlighted higher stability for copper(II) complexes vs magnesium ones, rising questions about the effective form of active species.